1st International & 28th National Conference on Nuclear Science & Technology 2022 (ICNST22)
Nuclear Science & Technology Research Institute

Evaluation of the secondary particles and prompt gamma production for proton range monitoring

Ramezanipour A., Taherparvar P*

[1]Department of Physics, University of Guilan, P.O. Box: 41335-1914, Rasht, Guilan

* *Email: p.taherparvar@guilan.ac.ir*

Abstract

In proton therapy, due to the high energy of the proton beam, different isotopes, neutrons, and photons are produced. In this paper, we evaluate the proton dose profile and secondary particle distribution (such as ^{11}C, ^{15}O, and neutrons), along with the prompt gamma distribution produced in the interaction of proton beams with energies of 75, 125, and 200 MeV with a PMMA phantom by simulation of the interaction process with the GATE Monte-Carlo code. The simulation results show that neutrons emission peaks ahead of the Bragg peak. On the other hand, the spatial distribution of the secondary particle distributions demonstrated that both prompt-gamma and positron emitter radionuclides have good correlation with proton dose distribution, then can be used for proton range evaluations by dedicated imaging systems.

Keywords: Proton Therapy, Secondary Particles, Prompt Gamma, GATE

Introduction

Today, proton therapy is used as one of the most important techniques in the treatment of various cancers. In this technique, with the interaction of high-energy protons with a specific tissue, a fraction of the beam particles will experience nuclear interactions that release secondary particles, photons, and neutrons with different energies [1]. The produced neutrons can move far distances from the production location and deposit their energies in the nearby healthy organs [2]. The secondary gammas, which are produced by proton-nucleus interactions, are classified into two separate types: characteristic prompt gammas (PGs) and positron annihilation gammas (PA), which are generated by positron emitter radionuclides [3]. In proton therapy, online range monitoring is an important step to provide early treatment assessment. Since the produced positron emitter nuclides have relatively long half-lives in comparison with treatment time, PET imaging is not considered a good technique for real-time monitoring of proton range [4]. An alternate method is based on the detection of the prompt gammas. In this study, by simulation of the proton beam interaction with a PMMA phantom by GATE code and evaluation of the spatial distribution of the secondary particles and produced photons, we demonstrate that the prompt gammas distribution has a close correlation with proton energy deposition profile at the Bragg peak position.

Materials and Methods

In the present study, a PMMA phantom with a dimension of 400×400×400 mm^3 was simulated. We defined a cylindrical proton beam with 3 cm diameter with uniform energy distribution with energies of 75, 125, and 200 MeV moving along the z-axis, using GATE code. The distance between source and phantom was 1m. Ten million particles to reach the statistical uncertainty of about 4% for the dose calculation. The simulations were performed with the QGSP-BIC-HP-EMZ physics list. The distribution of the secondary particles consist of positron emitter radioisotopes, neutrons, along with the emission of prompt gamma production by proton-nucleus interactions with the medium during proton therapy were studied, considering voxel dimensions of 1 mm^3. Moreover, the gamma spectrum generated by the interaction of protons with medium PMMA phantom was examined.

Results and discussion

At first, we measured the proton Bragg peak positions for the proton beams with energies of 75, 125, and 200 MeV, which were about 36, 94, and 215 mm, respectively (Table 1). Then, the β^+ emitters (^{11}C and ^{15}O) production profiles were obtained by GATE code in the PMMA phantom for proton energies of 75, 125, and 200 MeV (Figure 1-a, b, and c, respectively). Results show that the position of appearing peaks for ^{11}C and ^{15}O is approximately located at the proton Bragg peak positions in all cases and occurs at closer distances. As neutrons are the biggest source of photon contamination, we show the neutrons emitted length distribution due to the interaction of the protons with the PMMA phantom in Figure 2, for three different energy of the proton beams. For comparison purposes, the scaled Bragg peak curves have been shown in the figure. A continuous curve is seen for the neutron production in the medium. As shown in this figure, there is a weak correlation between the neutron production profile peaks and the proton Bragg peak.

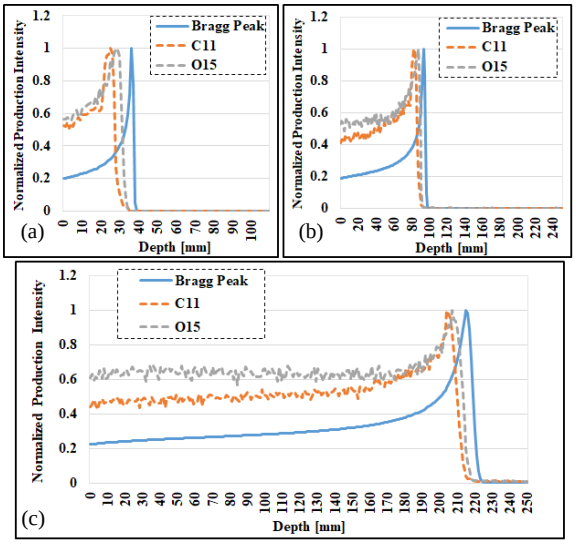

Figure 1. Isotope production for 75 MeV (a), 125 MeV (b), and 200 MeV (c) in the target, along with the representation of the related scaled Bragg peaks. The curves are scaled to allow proper presentation.

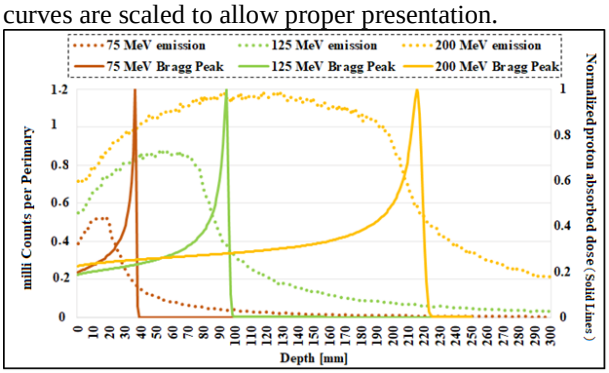

Figure 2. Neutron emission in the phantom, along with the representation of the related scaled Bragg peaks.

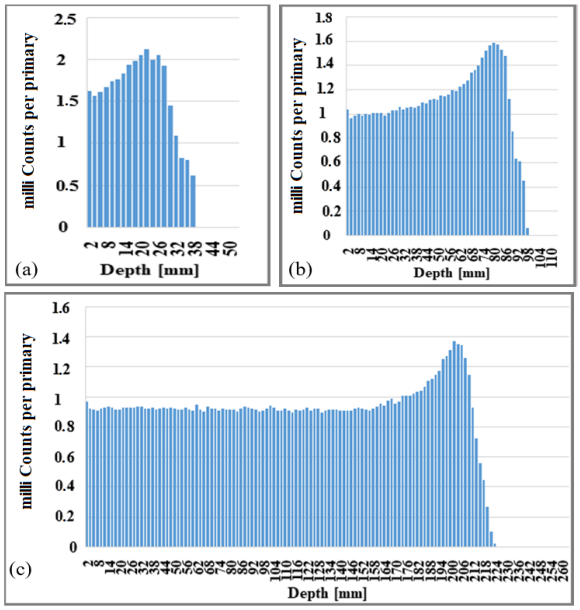

Figure 3. Histogram reperesentation of the prompt gamma emission for 75 MeV (a), 125 MeV (b) and 200 MeV (c) protons in the PMMA phantom.

Table 1. Production peak position for ^{11}C, ^{15}O, and prompt gamma.

	Production peak position (mm)		
Proton energy	75 MeV	125 MeV	200 MeV
Proton peak	36	94	215
^{11}C	25	83	204
^{15}O	28	87	207
Prompt gamma	25	83	202

Figure 3 shows the simulated prompt gamma emission length profile for different proton energies. The emission length profile follows the proton energy deposition and peaks, as presented in Table 1. The photon curves drop sharply before the Bragg peak and proton range position. Furthermore, results show the correlation between the prompt gamma production and the proton Bragg peak.

Conclusions

The present study has provided the secondary particle distribution, which can be used for PET imaging systems, and prompt gamma, which can be used for PGs imaging systems. Results show that the high neutron flux will maintain to be a challenge for every detection system, but discrimination techniques can reduce these effects. Evaluation of the secondary particle production shows that the production of ^{11}C and ^{15}O radioisotopes, as positron emitter radioisotopes, decreases near the Bragg peak dose curve to zero. On the other hand, prompt gamma emission spectrum continues to the low energy regions, below a few MeV. It is due to photons produced by inelastic proton interactions with a continuous low energy spectrum. There is a good correlation between the prompt gamma production and the proton Bragg peak in all proton energies. Moreover, the recorded prompt gamma photons were greater than the number of positron radioisotopes, which is a real advantage for proton range monitoring. Simulation results of the secondary particle distributions from proton interaction with the phantom show that both prompt-gamma and PET imaging can be used for in-vivo proton range measurements.

References

[1] Y. Chen, S. Ahmad, *Evaluation of inelastic hadronic processes for 250 MeV proton interactions in tissue and iron using GEANT4*, Radiat. Prot. Dosim., 136(1),11-16, (2009).

[2] S. B. Jia, et al., *Evaluation of energy deposition and secondary particle production in proton therapy of brain using a slab head phantom*, RPOR, 19(6), 376-384, (2014).

[3] J. C. Polf, et al., *Detecting prompt gamma emission during proton therapy: the effects of detector size and distance from the patient*, Phys. Med. Biol., 59(9), 2325-2340, (2014).

[4] G. Lönn, *In-beam proton range monitoring during proton therapy*, KTH Royal Institute of Technology, School of Engineering Sciences (2016).